Designing of a gasoline food-grade magnetic hammer mill

Mayowa Saheed Sanusi*, Musilu Olushola Sunmonu, Michael Mayokun Odewole, Obafemi Ibitoye Obajemihi, Abiola Lydia Adepoju, Sodiq Ayinde Olaleye

(Department of Food Engineering, Faculty of Engineering and Technology, University of Ilorin, Nigeria, and 240003.)

Abstract: This study aimed to design and fabricate a laboratory-scale gasoline food-grade magnetic hammer mill and to estimate the milling efficiency, milling yield, milling time, energy consumption, and energy intensity of some selected food materials (soybean, rice, and cassava flakes). The hopper, shaft, sieve, and hammers of the gasoline food-grade magnetic hammer mill are made of stainless steel and the structural base is made of mild steel. Cassava flakes had the highest milling yield (940 g), lowest energy consumption (0.94 MJ), energy intensity (0.94 MJ kg^{-1}), and the highest milling efficiency (94%) while soybean had the longest milling time (5.86 min). The cost of designing the gasoline food-grade magnetic hammer mill was estimated at $360. The designed gasoline food-grade magnetic hammer mill could be adopted for milling different food materials but its performance varies based on the food material. This hammer mill also serves as an alternative to the conventional electrically powered hammer mill with a special feature of trapping metallic object from food materials.

Keywords: energy consumption, gasoline, magnetic, hammer mill, food materials

Citation: Sanusi, M.S., M.O. Sunmonu, M.M. Odewole, O. I. Obajemihi, A.L. Adepoju, and S. A. Olaleye. 2022. Designing of a gasoline food-grade magnetic hammer mill. Agricultural Engineering International: CIGR Journal, 24(4): 195-208.

1 Introduction

Size reduction is widely used in the food industry operation to obtain smaller particle sizes out of larger particle sizes of the same material. In processing food materials, particle size reduction is an essential step; therefore, it is necessary to have an efficient means of achieving such goals, especially in developing countries. The sizes of food materials can be reduced by using different kinds of milling machines such as roller mill, pin mill, disc mill, and hammer mill (Yung et al., 2018). Hammer mills are commonly utilized in feed mills because they are easy to operate and maintained to produce desirable products (Manaye et al., 2019). Milling of food materials is a method of grinding them into flour or meal (Kawuyo et al., 2014). Hammer mill is a machine used for grating or crushing aggregate material into smaller pieces by repeated blows of the little hammer. It is designed and fabricated for grinding; processing and sieving all kinds of cereal, grains, and legumes such as maize, rice, wheat, millet, and soybean and it can also process different kinds of dried tubers such as dried cassava pieces (Ojomo and Fawohunre, 2020). According to Ajayi et al. (2019), hammer blades are driven by two or more sets of V-belts that link the prime mover and the mill. It is a tool or device which consists: of a

Received date: 2022-01-26 **Accepted date:** 2022-05-19

***Corresponding author: Sanusi Mayowa Saheed**, Ph.D., Department of Food Engineering, University of Ilorin, Nigeria, +2348069430996, Sanusi.ms@unilorin.edu.ng.

rotating head, and a set of swinging hammers (beaters) that breaks down and reduces food materials to predetermine sizes through a sieve. The food materials are pulverized as it enters the hammer mill by a combination of hammer blows and impact with the walls of the hammer mill. The food materials remain in the grinding chamber until they can pass through the sieve covering the discharge area (Hadi et al., 2017). A hammer mill is essentially a steel drum containing a vertical or horizontal rotating shaft or drum on which hammers are mounted. The hammers are free to swing on the ends of the cross, or fixed to the central rotor. The hammer mill can be used as a primary, secondary, or tertiary crusher.

Ajaka and Adesina (2014) developed a laboratory-size hammer mill for crushing minerals of medium hardness like dolomite, granite, and other materials with similar hardness. The mill was powered by electricity and could crush minerals to fine particles using different sieve sizes. Ezurike et al. (2018) designed a hammer mill made of major crushing components with high-speed rotating disc and flat-screen hammers for milling maize. The throughput of the machine was 31 kg h^{-1} at an efficiency of 93%. Ajayi et al. (2019) developed a blender-hammer crushing machine (2880 rpm hammer speed) for the production of fine paste and coarse products by using an electric motor of 3.75 kW, which gave a maximum throughput of 7.49 kg h^{-1} in milling cassava. Ojomo and Fawohunre (2020) also developed a hammer mill with double sieves for crushing maize with moisture content at a range of 8% – 16% wet basis. A crushing capacity of 51.5 kg h^{-1} was obtained, and the report showed that the milling power and specific energy requirement were dependent on the moisture content of maize. However, despite the tremendous work that has been done by researchers, literature is sparse on the design of a laboratory-scale hammer mill that is embedded with magnetic food-grade material. Literature on this kind of machine that uses gasoline as its main source of energy is also minimal. The design of a laboratory-scale gasoline food-grade magnetic hammer mill could aid in addressing the issue of production down-time that might occur as a result of sporadic power supply in developing countries. Also, the magnet in the machine due to its magnetic force of attraction (Young and Freedman, 2012), would assist in preventing metal objects from falling into the milling chamber thus aiding the milling of metal-free products. Therefore, this study aimed to design and fabricate a laboratory-scale gasoline food-grade magnetic hammer mill vis-a-vis evaluating the milling efficiency, milling yield, and milling time of some selected food materials (soybean, rice, and cassava flakes), and to determine the energy consumption and energy intensity of these food materials.

2 Materials and methods

2.1 Construction location

The design and fabrication of a laboratory-scale food-grade magnetic hammer mill was carried out at the Engineering Central Workshop, University of Ilorin (longitude: 8.48337 N, latitude: 4.67609 E), Nigeria. The performance evaluation and analyses were carried out at the Department of Food Engineering Pilot Plant II (longitude: 8.48328 N, latitude: 4.67675 E), University of Ilorin, Nigeria between October 2021 and November 2021.

2.2 Description of gasoline food-grade magnetic hammer mill

The gasoline food-grade magnetic hammer mill consists of a shaft, a control ON/OFF switch, a magnetic trap, hammers, gasoline engine, bolts and nuts, shaft, belt, hopper, sieve, pulley, and a structural base. The hopper, shaft, and hammers are made of stainless steel and the structural base is made of mild steel. The gasoline engine is mounted on the structural base; it uses a gravity feeding system where machines solely depend on the gravitational force. It is this force that helps to feed the food materials into the milling chamber. The control switch is used to control the engine speed, the machine which has sixteen (16) hammers of 0.18 kg each with a rotation speed of 11.3 m s^{-1} was used to mill food materials. The hammers are mounted on horizontal shafts where they rotate in a clockwise direction which depends on the direction of the rotor rotation; a rotor is a rotating shaft coupled to a gasoline motor engine. The hammers are driven by a belt; the belts cushion the motor from shock and allow for accurate speed adjustment. A stainless-steel sieve is placed within the milling chamber where the milled food material passes through; the sieve is detachable and this permits the use of various sizes of the sieve. The sieve type is a function of the size of the particles to be milled. A detailed description of the gasoline food-grade magnetic hammer mill's components is presented in the subsequent section

2.3 Gasoline food-grade magnetic hammer mill components

2.3.1 Hopper

This is the pathway through which the food materials were fed into the hammer mill. Inside the hopper, there is a stopper that regulates the flow of feed into the crushing chamber of the hammer mill.

2.3.2 Hammers

The hammers are rectangular stainless-steel metals that crush the food material fed into the crushing chamber and are attached to the shaft. There are sixteen hammers used for the mill. Each hammer is 10 mm thick which swings to enhance flexible operation.

2.3.3 Throat with magnetic embedment

This provides the passage for the food materials to be milled into the crushing chamber. The magnetic chamber is filled with high attraction magnets which help in trapping all ferrous material from the product to be milled to prevent it from entering the crushing chamber.

2.3.4 Shaft

This is a rod that holds the circular discs and these circular discs carry the hammers.

2.3.5 Crushing chamber

This unit houses the rotor that holds the hammers and the sieve for sieving. The inner part of the chamber is made from magnet of 10" × 10" × 7" that traps any metal object that might be present in the food material feed into the machine.

2.3.6 Sieve

The sieve act as a sieve for milled material before it is finally discharged. It is made up of stainless steel with a 6 μm mesh size and it is replaceable with other sizes.

2.3.7 Flange bearings

The bearings provide sliding motion, thus enabling smooth transport of the food materials from the main shaft to the shaft holding the hammers.

2.3.8 Discharge pipe

This is a pipe-like structure through which the milled food material is discharged.

2.3.9 Support stand structure

This is the stand that provides support for the whole machine and is made up of mild steel. It was made of 2 inches by 2 inches angle iron.

2.3.10 Gasoline engine (GX200)

The gasoline engine was used as the prime mover of the machine through a belt transmission.

2.3.11 Pulleys

Two pulleys were used for the machine which were the driver and the driven pulleys respectively. The driver pulley is mounted on the mechanical drive gasoline engine while the driven pulley was mounted on the rotor of the hammer mill machine.

2.4 Design and calculation

The general design was based on the process of allowing strong and durable metallic objects inform of a hammer to beat any material that obstructs its way during operation. The beating action of the hammers crushed food materials after being fed into the machine. This operation can also be referred to as size reduction or comminution. Figures 1-5 show the exploded view, top view, isometric view, front view, and side view of the gasoline food-grade magnetic hammer mill. Plate 1 shows the pictorial view of the developed gasoline food-grade magnetic hammer mill.

2.5 Determination of hopper volume

The volume (V_h) of the hopper was calculated using Equation 1

$$V_h = A \times H \tag{1}$$

where, A (mm^2) is the area of the hopper and H is the height between the hopper ends (50 mm)

The area of the hopper (A) was calculated using Equation 2.

$$A = \frac{1}{2}(a + b) \times h \tag{2}$$

where, a is the top width of the hopper (100 mm), b is the base width of the hopper (205 mm) and h is the side length of the hopper (225 mm).

$A = 34312.5\ mm^2 \approx 0.0343\ m^2$

Therefore, by substituting Equation 2 in Equation 1, the hopper volume is estimated as 0.00172 m^3**.**

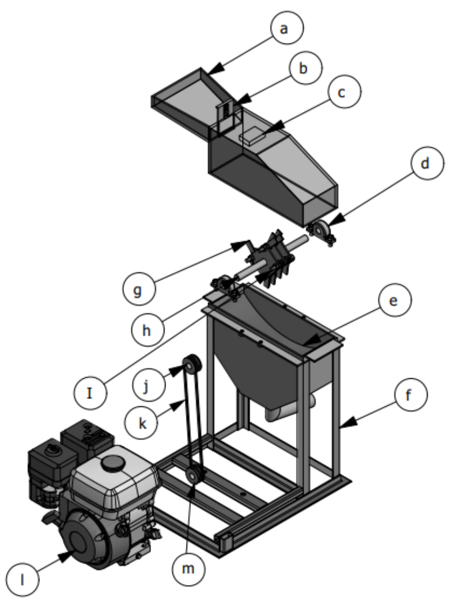

PARTS LIST			
ITEM	QTY	PART NAME	DESCRIPTION
a	1	HOPPER	
b	1	STOPPER	
c	1	MAGNET	
d	1	FLANGE BEARING	
e	1	SIEVE	
f	1	SUPPORT FRAME	
g	16	HAMMER(BEATERS)	
h	1	SHAFT	
I	8	BOLTS	
j	1	DRIVEN PULLEY	
k	1	BELT	
l	1	GASOLINE ENGINE	GX 200
m	1	DRIVER PULLEY	

Figure 1 Exploded view of the gasoline food-grade magnetic hammer mill

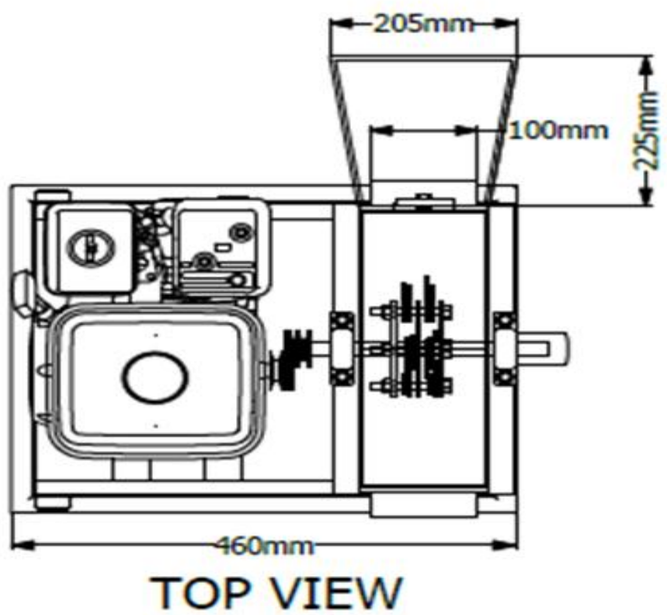

Figure 2 Top view of the gasoline food grade magnetic hammer mill

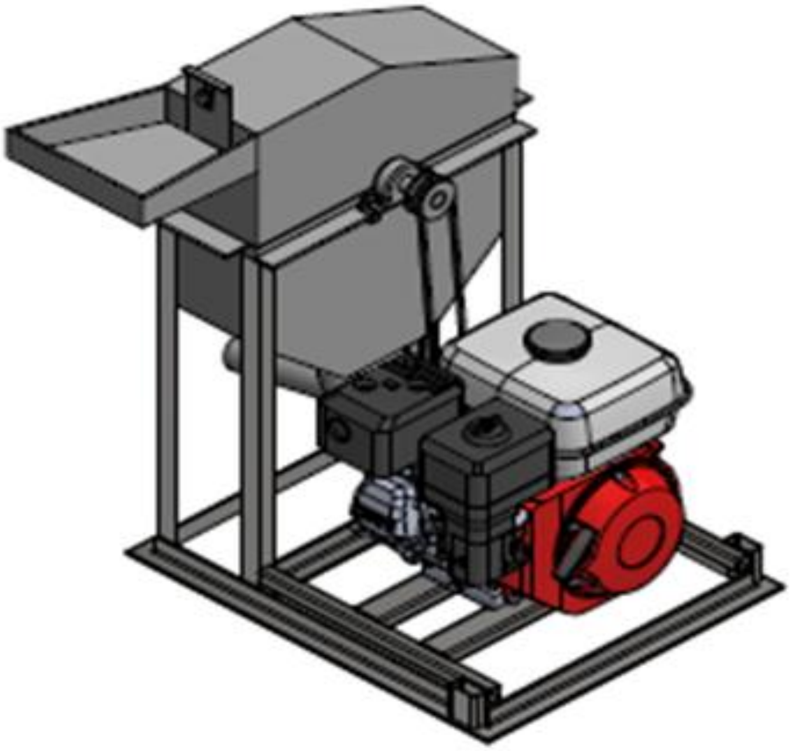

Figure 3 Isometric view of the gasoline food grade magnetic hammer mill

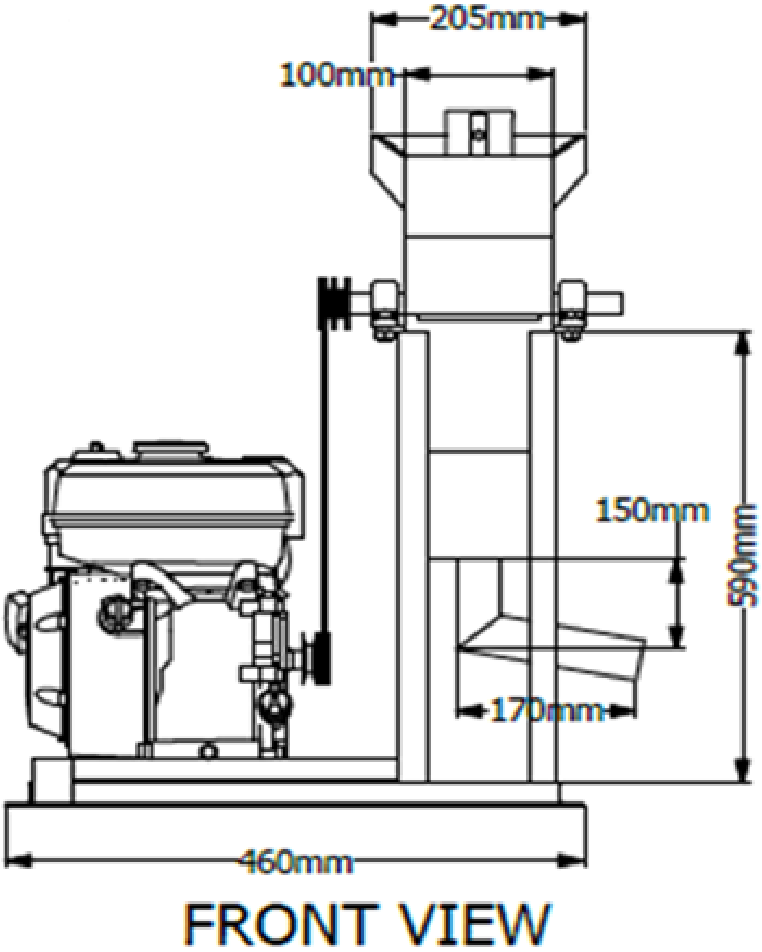

Figure 4 Front view of the gasoline food grade magnetic hammer mill

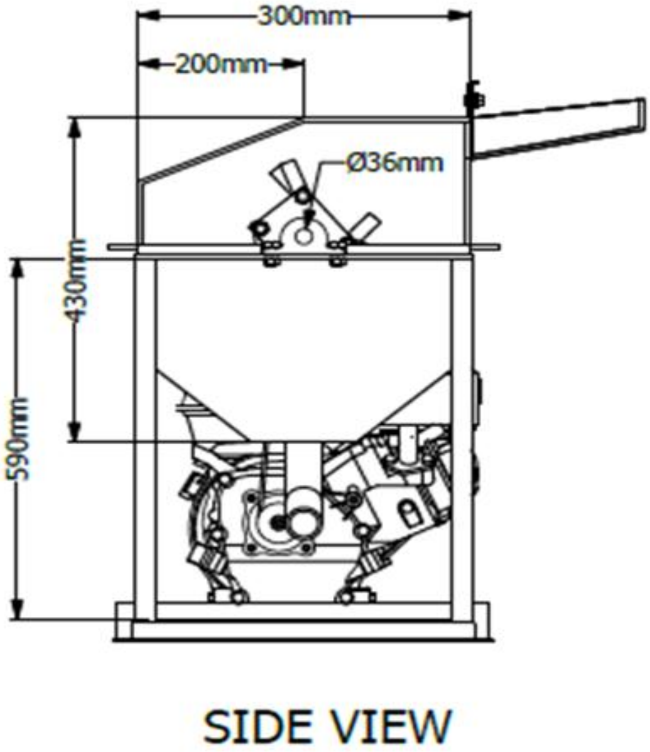

Figure 5 Side view of the gasoline food grade magnetic hammer mill

Plate 1 Pictorial view of the developed gasoline food-grade magnetic hammer mill

2.7 Determination of shaft speed

The speed of the shaft used was determined using information obtained from the diameters of the driving and driven pulley and the revolution of the driving pulley. The number of revolutions of the driven pulley N_2 was achieved by using Equation 3 as described by Spolt (1988).

$$\frac{D_1}{D_2} = \frac{N_2}{N_1} \quad (3)$$

where, D_1 is the diameter of the driving pulley ($60\ mm$), D_2 is the diameter of the driven pulley ($90\ mm$) and N_1 is the number of revolutions of the driving pulley ($3600\ rpm$) by the gasoline engine. Therefore, the number of revolutions of the driven pulley N_2 is $2400\ rpm$.

2.8 Determination of the length of belt

The length of the belt was calculated using Equation 4 as described by Patton (1980).

$$L = 2C + \frac{\pi}{2}(D_1 + D_2) + \left(\frac{D_1 - D_2}{4C}\right)^2 \quad (4)$$

where, L is the length of the belt, π is 3.142 and C is the centre between the two shafts ($390\ mm$).

$L = 1015.65\ mm$

2.9 Belt contact angle

The belt contact angle (α) can be calculated using Equation 5 as described by Morakinyo et al. (2014)

$$\alpha = \sin^{-1}\left(\frac{R - r}{C}\right) \quad (5)$$

where, R is the radius of the driven pulley ($45\ mm$) and r is the radius of the driving pulley ($30\ mm$). Therefore, the belt contact angle is 2.20°.

2.10 Angle of wrap around each pulley

The angle of wrap around each pulley (the driving and driven) was calculated using Equations 6 and 7 respectively by Ezurike et al. (2018).

$$\theta_1 = 180° + 2\alpha \quad (6)$$

$$\theta_1 = 184.4°$$

$$\theta_2 = 180° - 2\alpha \quad (7)$$

$$\theta_2 = 175.6°$$

Therefore, θ is the average angle of wrap around each pulley (the motor and the shaft) in radian from Equations 6 and 7.

$$\theta = \frac{\left(184.4 \times \frac{\pi}{180}\right) + (175.6 \times \frac{\pi}{180})}{2}$$

Therefore, θ was 3.14°. The coefficient of friction (μ) between belt pulleys was assumed to be 0.3 (Flavel and Rimmer, 1981).

2.11 Mass of hammer

The mass of a unit hammer (M_h) was weighed to be 0.18 kg and there are sixteen (16) hammers. Therefore, the total mass (T_m) of the hammers was determined using Equation 8 as described by Hannah and Stephens (1984).

$$T_m = M_h \times g \quad (8)$$

where, M_h is the mass of the hammer (2.88 kg) and g is the acceleration due to gravity (9.81 ms^{-2}). Therefore, T_m is 28.25 N.

2.12 Velocity of the shaft

The velocity of the shaft (v) was calculated using Equation 9 (Khurmi and Gupta, 2005).

$$v = \frac{\pi N D}{60} \quad (9)$$

where, N is the number of revolution (2400) of the driven pulley and D is the diameter of the driven pulley ($0.09\ m$). Therefore, the velocity of the shaft is equivalent to $11.3\ ms^{-1}$.

2.13 Centrifugal force exerted by the hammer

The centrifugal force (F_c) exerted by the hammer was calculated using Equation 10 as described by Hannah and Stephens (1984).

$$F_c = \frac{mv^2}{rs} \quad (10)$$

where, m is the total mass of the hammer $2.88\ kg$, rs is the radius of the shaft (0.018 m) and v is the velocity of the shaft ($11.3\ ms^{-1}$).

$F_c = 20.43\ kN$

2.14 Determination of tensions on the belt

According to Khurmi and Gupta (2005), the density of belt (rubber) is given as 1140 kg m^{-3} Therefore, the tension on each side of the belt was calculated using Equations 11 and 12 by Ezurike et al. (2018).

The tension on each side of the belt was calculated using Equation 11.

$$\frac{T_1 - T_c}{T_2 - T_c} = e^{\mu\theta} \quad (11)$$

where, T_1 is the tension on the tight side of the belt, T_2 is the tension on the slack side of the belt, T_c is the centrifugal tension on the belt, μ is the coefficient of friction between the belt and pulley and θ is average angle of wrap around each pulley.

$$T_c = Mv^2 \quad (12)$$

where M is the mass of the belt per unit length and v is the velocity of the shaft.

Also, the centrifugal tension can be calculated using Equation 13 as described by Ezurike et al. (2018).

$$T_c = \frac{T_1}{3} \quad (13)$$

The mass of the belt per unit length (M) was calculated using Equation 14 by Morakinyo et al. (2014). Where w is the width (12 mm), t is the thickness ((9 mm) x belt density), and ρ is the density of the belt (1140 kgm^{-3})

$$M = w \times t \times \rho \quad (14)$$

$$M = 0.123\ kgm^{-1}$$

From Equation 12, the centrifugal tension obtained was 15.7 N.

From Equation 13, $T_1 = 3T_c$ $T_1 = 47.1\ N$

From Equation 11,

$$\frac{47.1-15.7}{T_2 - 15.7} = e^{0.3\times3.14} \quad T_2 = 27.78\ N$$

2.15 Determination of power transmitted by the belt

The power transmitted by the belt was calculated using Equation 14 by Khurmi and Gupta (2005).

$$P = (T_1 - T_2)v \quad (14)$$

$$P = 218.32\ W$$

2.16 Performance evaluation

The designed gasoline food-grade magnetic hammer mill was evaluated based on the determination of the milling efficiency, milling yield, and milling time of 1 kg each of soybean, rice, and cassava flakes. The selected food materials' moisture content (wb) was determined using a moisture analyzer (Model No: LSC-50, China). The moisture contents of the soybean, rice, and cassava flakes samples were 18%, 14%, and 10%, respectively. The milling efficiency and milling yield were determined using Equations 15 and 16 while the milling time was determined by monitoring and noting the average time taken to crush the mass of food material fed efficiently. A timer (Diamond mechanical stopwatch, Model 504, China) was used to monitor the time used. The food materials were slowly fed into the milling chamber through the hopper to prevent clogging the sieve. The process was repeated three times and the average reading was used to calculate the crushing efficiency of the machine for each material, the milling yield and milling time for each material.

The milling efficiency (ME) was determined using Equation 15 as described by Oluwole et al. (2019).

$$ME = \frac{M_2}{M_1} \times 100 \quad (15)$$

where, M_2 is the mass of the milled samples and M_1 is the mass of the raw samples (unmilled)

The milling yield (MY) was determined using Equation 16

$$MY = M_1 - M_2 \quad (16)$$

2.17 Energy consumption analysis

The energy consumption (EC) required during the milling of 1 kg each of soybean, rice, and cassava flakes into flour was estimated using the approach reported by Sanusi and Akinoso (2021) as shown in Equation 17. The energy intensity (EI) of the milling operation was determined using Equation 18.

$$EC = \left(0.75N_p \times 0.0167t\right) + (Q_f \times C_f) \quad (17)$$

Average manpower in the tropical region (0.75 MJ), N_p is the number of the person performing the milling operation, C_f is the calorific value of gasoline (45 MJ) and Q_f is the quantity of gasoline used during milling which was measured by taking the mass of gasoline before and after use for each sample, t is the time taken for the milling process and m is the mass of the samples before milling.

$$EI = \frac{EC}{m} \quad (18)$$

2.18 Statistical Analysis

All determinations were performed in triplicate (n=3). All data were subjected to a one-way analysis of variance (ANOVA) and means were separated using Duncan's Multiple-Range Test (DMRT) at $p < 0.05$.

3 Results and discussion

3.1 Milling efficiency

The milling efficiencies of soybean, rice, and cassava flakes were observed to be 73%, 88%, and 94% respectively as shown in Figure 6. There was a significant difference at $p \leq 0.05$ in the milling efficiency of soybean, rice and cassava flakes. The differences in milling efficiency could be due to the difference in textural properties of the samples. The lower milling efficiency for soybean could be due to the harder texture and higher moisture content of the soybean. Moon and Yoon (2017), reported that the efficiency of the milling process increases as moisture content decreases. In addition, Lyu et al. (2020) reported that a hammer mill is highly suitable for grinding fibrous materials and this could be the further reason why the milling efficiency of cassava flakes and rice is higher than soybeans.

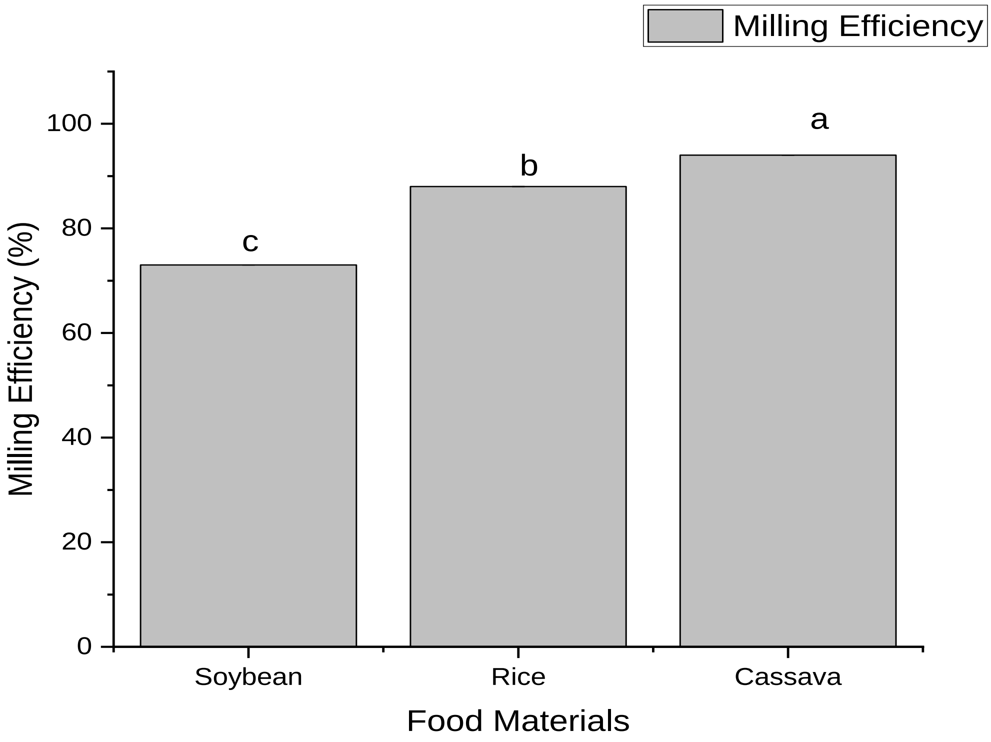

Figure 6 Milling efficiency of soybean, rice, and cassava flakes. Graph bars with different superscripts (a, b, and c) indicate significant differences among the food materials with the milling efficiency (p <0.05)

3.2 Milling yield

The milling yield of soybean, rice, and cassava flakes is shown in Figure 7. It was observed that the milling yield was 730 g, 880 g, and 940 g respectively. There was a significant difference at $p \leq 0.05$ in the milling yield of soybean, rice and cassava flakes. The differences in milling yield could be due to the particle size and the moisture content of the milled samples. There was a higher yield in the milling of cassava flakes due to its soft texture and lower moisture content. The lower yield obtained in the milling of soybean was due to higher moisture content in soybean and this led to the stickiness of the flour on the wall of the hammer mill. This result is in agreement with the report of Lyu et al. (2020), which stated that the particle size and shape of material influence its yield.

3.3 Milling time

Figure 8 shows the milling times of soybean, rice and cassava flakes. The milling time for soybean, rice and cassava flakes were observed to be 5.86, 4.25 and 3.22 min respectively. There was a significant difference at $p \leq 0.05$ in the milling time of soybean, rice and cassava flakes. The difference in milling time could be due to the difference in the textural behaviour of the samples during milling.

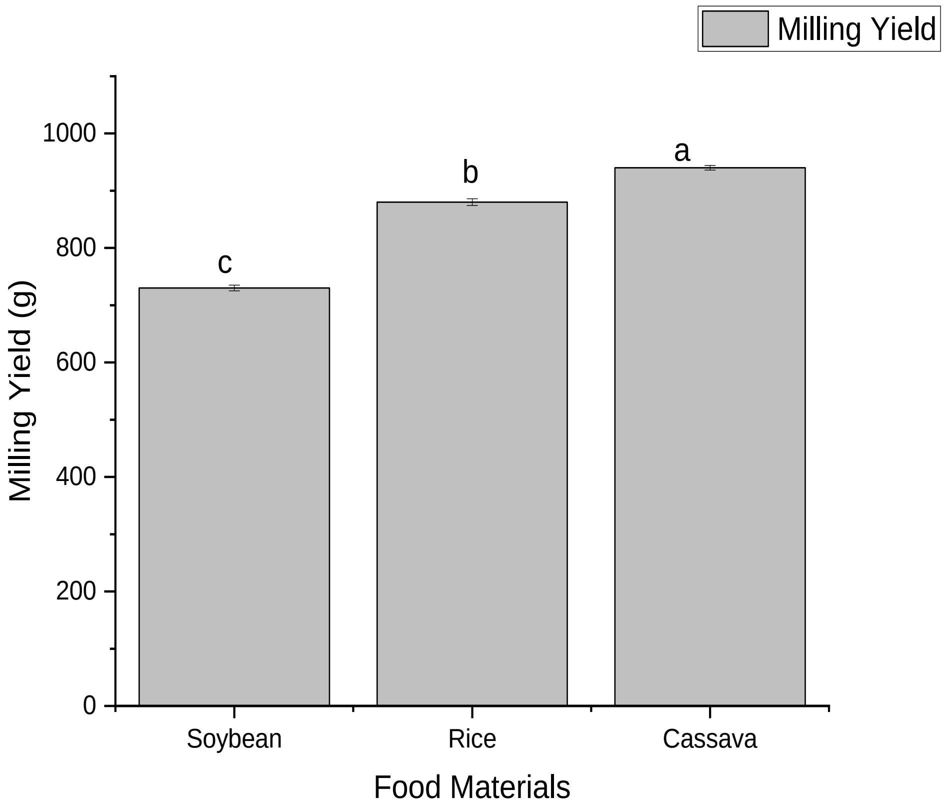

Figure 7 Milling yield of soybean, rice and cassava flakes. Graph bars with different superscripts (a, b and c) indicate significant differences among the food materials with the milling yield (p < 0.05)

Figure 8 Milling time of soybean, rice and cassava flake. Graph bars with different superscripts (a, b and c) indicate significant differences among the food materials with the milling time (p < 0.05)

3.4 Energy consumption

The energy consumption during the milling of soybean, rice, and cassava flakes were observed to be 2.10, 1.62, and 0.94 MJ respectively as shown in Figure 9. There was a significant difference at $p \leq 0.05$ in the energy consumption of soybean, rice, and cassava flakes. The difference in energy consumption could be due to the milling time, the quantity of gasoline consumed during the milling operation and the textural properties of each sample. It was observed that soybean consumed more energy because it was milled for longer time which led to higher gasoline consumption and also had higher moisture content. An increase in moisture content increases energy consumption during size reduction (Miao et al., 2011). Sanusi and Akinoso (2020), also reported that milling duration have an influence on energy consumption.

3.5 Energy intensity

The energy intensity during the milling of soybean, rice and cassava flakes were observed to be 2.10, 1.62 and 0.94 MJ kg^{-1} respectively as shown in Figure 10. There was a significant difference at $p \leq 0.05$ in the energy intensity of soybean, rice and cassava flakes. The differences in energy intensity are due to differences in energy consumption for each sample. The lowest energy intensity in cassava flakes could be due to its lower milling duration which led to lower gasoline consumption.

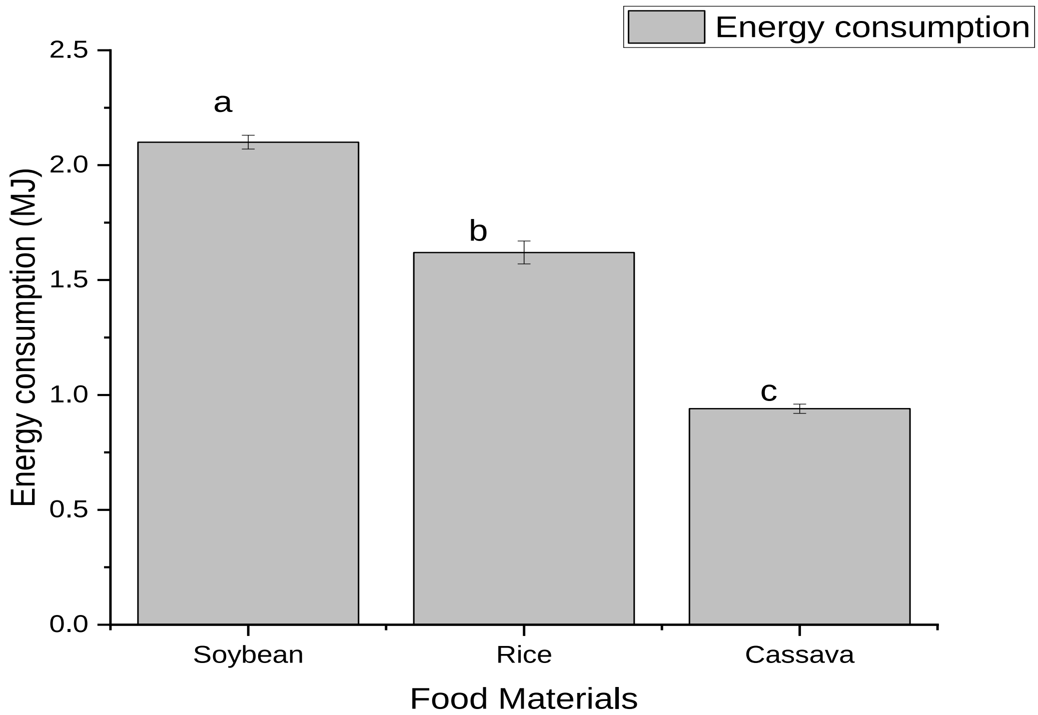

Figure 9 Energy consumption of soybean, rice and cassava flake. Graph bars with different superscript (a, b and c) indicate significant differences among the food materials with the energy consumption ($p < 0.05$)

3.6 Bill of engineering measurement and evaluation of the designed gasoline food-grade magnetic hammer mill

Table 1 shows the bill of engineering measurement and evaluation of the designed gasoline food-grade magnetic hammer mill. An estimated $360 was spent as the cost of purchasing the required materials for the fabrication of the hammer mill and also for the miscellaneous.

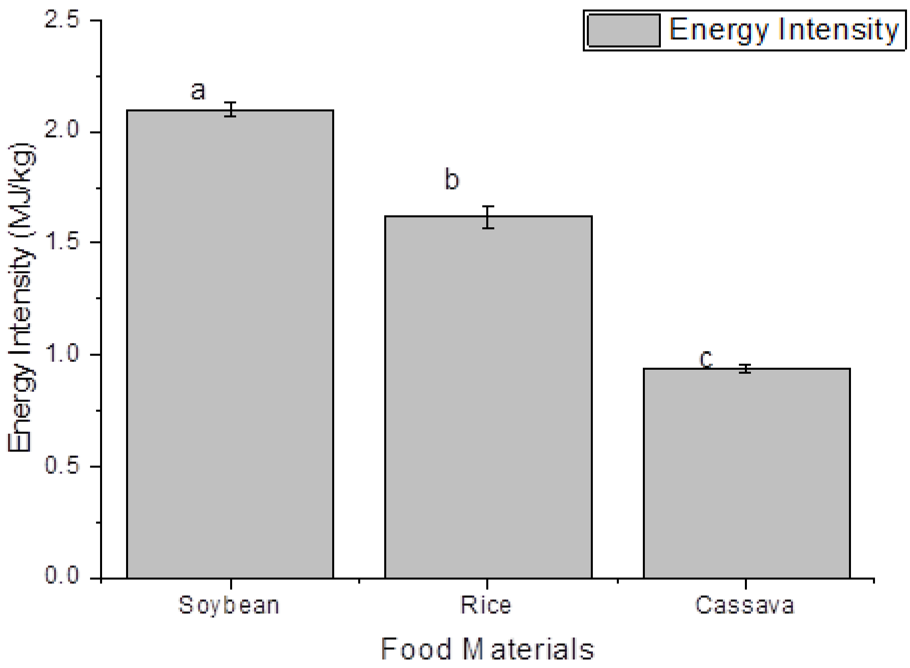

Figure 10 Energy intensity of soybean, rice and cassava flake. Graph bars with different superscript (a, b and c) indicate significant differences among the food materials with the energy intensity (p < 0.05)

Table 1 Bill of Engineering Measurement and Evaluation (B.E.M.E) for the gasoline food-grade magnetic hammer mill

S/N	Material Description	Material Specification	Quantity	Total Cost ($)
1	Stainless steel plate	2.8 mm thickness		96.58
2	Support stand	Vertical, 2ft	4	28.97
		Horizontal, 15.5 mm	2	
		Horizontal, 4.5 mm	2	
3	Pulley	Driven, 6 mm × 9 mm	1	7.24
		Driving, 2"	1	6.04
4	Mesh	0.6 μm	1	3.62
5	Shaft	1ft × 25 mm	1	12.55
6	Gasoline motor	6.5 Hp	1	82.09
7	Hammer	Tip, 0.5 mm circumference,	16	19.32
		mass of hammer, 0.18 kg		
8	Belt	12 mm thickness	1	1.81
		9 mm width		
9	Bolt and Nut	Size 16	10	6.04
		Size 13	4	3.62
10	Angle iron			13.65
11	Bearing			6.04
12	Magnet	10"× 10"× 7"	1	4.83
13	Workmanship			48.29
14	Transportation			12.07
15	Painting	Silver colour	2	4.83
17	Gasoline			2.41
	Total			360.00

4 Conclusions

A laboratory gasoline food-grade magnetic hammer mill was successfully designed and can be scale-up for commercial purposes. The designed machine is capable of milling grains, legumes, and tubers products. From the design consideration and analysis, portability, reliability, safety, and serviceability were given due consideration. The machine was designed to use gasoline (premium motor spirit) as its main source of energy. The cost of designing of the gasoline food-grade magnetic hammer mill was estimated at $360. The average milling efficiency, milling yield, milling time, energy consumption and energy intensity for soybean, rice and cassava flakes varies. Cassava flakes had the highest milling efficiency and milling yield. Also, the energy consumption, energy intensity and milling time were lower in the milling of cassava flakes when compare with rice and soybean. The gasoline food-grade magnetic hammer mill could serve as an alternative to the unreliable conventional electrical source in developing countries and can also trap any metal object that might be present in the raw material.

Conflict of interest

The authors declared that there is no conflict of interest.

References

Ajaka, E. O., and A. Adesina 2014. Design, fabrication and testing of a laboratory size hammer mill. *International Journal of Engineering and Advance Technology Studies*, 2(2): 11-21.

Ajayi, C. O., F. A. Oyawale, and S. A. Afolalu. 2019. Development of blender-hammer mill for multipurpose use. *Journal of Physics: Conference Series*, 1378(3): 032024.

Ezurike, B. O., O. J. Osazuwa, C. A. Okoronkwo, and K. I. Okoji. 2018. Design, construction and performance evaluation of a flat screen hammer mill machine. *African Journal of Science, Technology, Innovation and Development*, 10(6): 683-690.

Flavel. M. D., and H. W. Rimmer. 1981. Particle breakage in an impact crushing environment. In SME-AIME Annual Meeting, 22-26. Chicago, IL, 22-26 February.

Hadi, M. I., M. A. Bawa, H. Dandakouta, M. Ahmed, and P. M. Kamtu. 2017. Improvement on the design, construction and testing of hammer mill. *American Journal of Engineering Research*, 6(3): 139-146.

Hannah, J., and R. C. Stephens 1984. Mechanics of machines, elementary theory and examples. Butterworth-Heinemann, 4th edition.

Kawuyo, U. A., M. N. Chineke, A. B. Ahmad, and E. O. Amune. 2014. Grain milling machine. Paper I: Design and Construction. *Arid Zone Journal of Engineering, Technology and Environment*, 10: 75-84.

Khurmi, R. S., and J. K. Gupta. 2005. *A Textbook of Machine Design*. 14th ed. Eurasia Publishing House (Pvt.) Ltd. Ram Nagar, New Delhi-110 055.

Lyu, F., M. Thomas, W. H. Hendriks, and A. F. B. Van der Poel. 2020. Size reduction in feed technology and methods for determining, expressing and predicting particle size: A review. *Animal Feed Science and Technology*, 261: 114347.

Manaye, W., B. Hailu, and T. Ashokkumar. 2019. Redesign and Fabrication of Hammer Milling Machine for Making Pasta. *International Journal of ChemTech Research*, 12(03):202-218.

Morakinyo, T. A., Ogunsina, B. S. and Adebayo, A. A. 2014. Adaptation of Impact Hammer Mill for Crushing Cocoa Pods Husk as a Livestock Feed Constituent. *Journal of Agricultural Engineering and Technology*, 22(3), 1-11.

Miao, Z., T. E. Grift, A. C. Hansen, and K. C. Ting. 2011. Energy requirement for comminution of biomass in relation to particle physical properties. *Industrial Crops and Products*, 33(2): 504-513.

Moon, J. H., and W. B. Yoon. 2017. Effect of moisture content and particle size on grinding kinetics and flowability of balloon flower (*Platycodon grandiflorum*). *Food Science and Biotechnology*, 27(3): 641-650.

Ojomo, O. A., and A. J. Fawohunre. 2020. Development of a hammer mill with double sieving screens. *European Journal of Engineering and Technology Research*, 5(5): 617-621.

Oluwole, F. A., A. Gujja, and A. K. Abubakar. 2019. Effect of number of beaters on the performance of household hammer mill. *Arid Zone Journal of Engineering, Technology and Environment*, 15(3): 619-627.

Patton, E. S. 1980. Mechanism Design Analysis. Prentice

Hall of India Private Ltd.

Sanusi, M. S., and R. Akinoso 2020. Multiobjective optimization of parboiled rice quality attributes and total energy consumption. *Nigerian Journal of Technological Research*, 15(3): 24-33.

Sanusi, M. S., and R. Akinoso. 2021. Modelling and optimising the impact of process variables on brown rice quality and overall energy consumption. *International Journal of Postharvest Technology and Innovation*, 8(1): 70-88.

Spolt, M. F. 1988. *Design of Machines Element*. 6th ed. New Delhi, India: Prentice Hall.

Young, H. D., and R. A. Freedman 2012. *University Physics with Modern Physics*. 13th ed. Sears, Francis Weston, United States of America: Pearson Education, Inc., publishing as Addison-Wesley.

Yung, H., Y. J. Lee, and W. B. Yoon. 2018. Effect of moisture content on the grinding process and powder properties in food: A review. *Processes*, 6(6): 69.